2010 IEEE International Conference on Robotics and Automation
Anchorage Convention District
May 3-8, 2010, Anchorage, Alaska, USA

Trajectory Generation with Natural ZMP References for the Biped Walking Robot SURALP

Evrim Taşkıran, Metin Yılmaz, Özer Koca, Utku Seven and Kemalettin Erbatur, *Member, IEEE*

***Abstract*—Bipedal locomotion has good obstacle avoidance properties. A robot with human appearance has advantages in human-robot communication. However, walking control is difficult due to the complex robot dynamics involved.**

Stable reference generation is significant in walking control. The Linear Inverted Pendulum Model (LIPM) and the Zero Moment Point (ZMP) criterion are applied in a number of studies for stable walking reference generation of biped robots. This is the main route of reference generation in this paper too.

We employ a natural and continuous ZMP reference trajectory for a stable and human-like walk. The ZMP reference trajectories move forward under the sole of the support foot when the robot body is supported by a single leg. Robot center of mass (CoM) trajectory is obtained from predefined ZMP reference trajectories by Fourier series approximation. We reported simulation results with this algorithm in our previous works. This paper presents the first experimental results. Also the use of a ground push phase before foot take-offs reported in our previous works is tested first time together with our ZMP based reference trajectory. The reference generation strategy is tested via walking experiments on the 29 degrees-of-freedom (DOF) human sized full body humanoid robot SURALP (Sabanci University Robotics Research Laboratory Platform). Experiments indicate that the proposed reference trajectory generation technique is successful.

I. Introduction

THE humanoid shape for a robot is suitable for obstacle avoidance purposes in the human environment. Robots in the human shape can be accepted as a social creature by human beings. Nevertheless, there are a variety of problems which should be alleviated for the realization of the human-robot coexistence. The bipedal free-fall manipulator is difficult to stabilize [1]. This makes the walking control a challenging problem. In biped robot systems, walking pattern is as important as balance control techniques.

The ZMP criterion is widely accepted as a stability measure for bipedal locomotion. This criterion states that, ZMP should lie within the supporting area of the feet during the walk [1]. This area defined by the borders of the feet in contact with the ground is often called the support polygon.

Manuscript received September 8, 2009. This work was supported by The Scientific and Technological Research Council of Turkey under Project Grant No. 106E040.

The authors are with the Faculty of Engineering and Natural Sciences, Sabanci University, Istanbul, 34956 Turkey (phone: +90-216-483-9585; fax: +90-216-483-9550; e-mail:, evrimt@su.sabanciuniv.edu, , metinyilmaz@ su.sabanciuniv.edu, ozerk@su.sabanciuniv.edu, utkuseven@ su.sabanciuniv.edu, erbatur@sabanciuniv.edu).

The ZMP coordinates are functions of the positions and accelerations of the links and the body of the humanoid robot. It is difficult to use these expressions of many variables in reference generation and control algorithm design. Dynamics equations of the free fall biped robot are complicated too and it is also not straight forward to have an insight from them to design stable references and stabilizing controllers. This is where an approximate model can prove much more useful than a detailed one. The LIPM [2] is such an approximate model of the legged robot. It consists of a point mass of constant height and a massless rod connecting the point mass with the ground. By virtue of this model, a quite simple relation between the ZMP and the robot CoM coordinates is obtained [3]. This relation is exploited for ZMP based stable walking reference generation in a number of studies. In such works, robot CoM trajectory is obtained from predefined stable ZMP reference trajectories. There is a freedom in choosing the ZMP reference as long as the criterion above is satisfied. A choice is to keep it fixed at the center of the foot sole when only one foot is supporting the body (single support phase) and interpolating between the foot centers when two feet support it (double support phase) [4]. However, human-like walk can be obtained by ZMP trajectories which move forward when the robot body is supported by a single leg [5-7]. A discussion on the definition of naturalness and performance of the walk can be found in [8].

In [8], Erbatur and Kurt introduce a forward moving discontinuous ZMP reference trajectory for a stable and human-like walk and as in [4] employ Fourier series approximation to obtain CoM reference trajectory from this ZMP trajectory. This method exploits the periodic nature of the steady walk trajectories as is done with Fast Fourier Transforms in an earlier work in [9]. The ZMP reference in the double support phases in [8] is obtained indirectly with a Lanczos smoothing, which also provides smoothing of the Gibbs phenomenon peaks due to Fourier approximation. Although the walk period is defined by the user, the partition of the period into the single and double support phases is due to the smoothing process, and not predefined. [10] uses a Fourier series approximation for the computation of the CoM trajectory from a given ZMP reference curve, too. However, it improves [8] by defining a continuous ZMP reference and the durations of the single and double support phases are fully pre-assigned. This is useful since these parameters play an important role in the parameter tuning in experiments as

[11, 12] suggest. The naturalness of the walk is preserved, in that the single support ZMP reference is forward moving. Also, the continuity of the introduced ZMP reference makes smoothing unnecessary.

This paper employs the CoM reference generation method of [10]. However, [10] justifies the applicability of the technique via simulations on a 12-DOF biped robot model, whereas we present experimental walking results obtained with the robot SURALP - a 29 DOF full-body bipedal humanoid robot designed and built at Sabanci University, Turkey [12]. In addition to experimental verification, a second contribution of this paper is the introduction of ground push phases in the z-directional foot references before foot take off instances. These phases, which are successful in initiating take-offs, were not used in [10].

The ZMP based CoM reference trajectory generation method as in [10] is discussed in the next section for the sake of completeness. The foot reference generation is presented in this section, too. The controller structure used in the experiments is summarized in Section III. Section IV presents the experimental results. This is followed by a conclusion in the last section.

II. ZMP Based Reference Generation

In place of using complex full dynamics models, the simple LIPM is more suitable for controller synthesis. A point mass is assigned to the CoM of the robot and it represents the body (trunk) of the robot. The point mass is linked to a stable (not sliding) contact point on the ground via a massless rod, which is idealized model of a supporting leg. In the same manner, the swing leg is assumed to be massless too. With the assumption of a fixed height for the robot CoM a linear system which is decoupled in the *x* and *y* directions is obtained. The system described above is shown in Fig. 1. $c = (c_x \quad c_y \quad c_z)^T$ is position of the point mass in this figure. The ZMP is defined as the point on the *x*-*y* plane on which no horizontal torque components exist. For the structure shown in this figure, the expressions for the ZMP coordinates p_x and p_y are [3]:

$$p_x = c_x - (z_c / g)\ddot{c}_x \tag{1}$$

$$p_y = c_y - (z_c / g)\ddot{c}_y \tag{2}$$

z_c is the height of the plane where the motion of the point mass is constrained and g is the gravity constant. A suitable ZMP trajectory can be generated without difficulty for reference generation purposes:

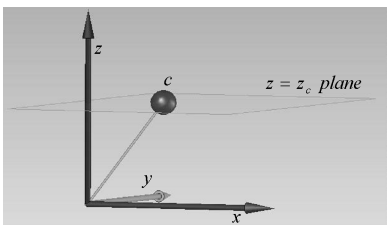

Fig. 1. The linear inverted pendulum model

As the only stability constraint, the ZMP should always lie in the supporting polygon defined by the foot or feet touching the ground. The ZMP location is generally chosen as the middle point of the supporting foot sole. In [4], the reference ZMP trajectory shown in Fig. 2 is created with this idea. Firstly, support foot locations are chosen. *A* in the figure is the distance between the foot centers in the *y* direction, *B* is the step size and *T* is the half of the walking period in this figure. The selection of support foot locations and the half period *T* defines the staircase-like p_x and the square-wave structured p_y curves. However, in [4], the naturalness of the walk is not considered. As mentioned above, in that work ZMP stays at a fixed point under the foot sole, although investigations in [5-7] show that the human ZMP moves forward under the foot sole. Fig. 2 also shows that the transition from left single support phase to the right single support phase is instantaneous. There exists no double support phase. In order to address the naturalness issue, the p_x reference (p_x^{ref}) curve shown in Fig. 3 is employed in [8]. In this figure, *b* defines the range of the ZMP motion under the sole. A trajectory symmetric in the x-direction, centered at the foot frame origin is assumed.

Having defined the curves, and hence the mathematical functions for $p_x^{ref}(t)$ and $p_y^{ref}(t)$, the next step is obtaining CoM reference curves $c_x^{ref}(t)$ and $c_x^{ref}(t)$ from $p_x^{ref}(t)$ and $p_y^{ref}(t)$, respectively. Position control schemes for the robot joints with joint references obtained by inverse kinematics from the CoM locations can be employed once the CoM trajectory is computed.

The computation of CoM trajectory from the given ZMP trajectory can be carried out in a number of ways [3, 4]. [4], for the reference ZMP trajectories in Fig. 2, proposes an approximate solution with the use of Fourier series representation to obtain CoM references. Taking an approach similar to the one in [4], [8] develops an approximate solution for the c_x and c_y references corresponding to the moving ZMP references in Fig.3. In this process Fourier series approximations of the ZMP references $p_x^{ref}(t)$ and $p_y^{ref}(t)$ and of the CoM references are obtained. Although the ZMP reference in the x-direction in Fig. 3 is forward moving and hence natural as desired, it is not continuous. So is the ZMP reference of Fig. 3 in the y-direction. The y-direction reference is in the form of a square wave as in Fig. 2. This discontinuous function corresponds to an instantaneous switching of the support foot, from right to left and from left to right foot, without an intermediate double support phase. [8] uses Lanczos sigma factor smoothing for i) Suppressing the Gibbs phenomenon, ii) Introducing double support phases. This, however, introduces problems too: Gibbs suppression and double support period determination are coupled. However, having the single and double support periods as freely adjustable parameters plays a vital role in tuning of the walking pattern.

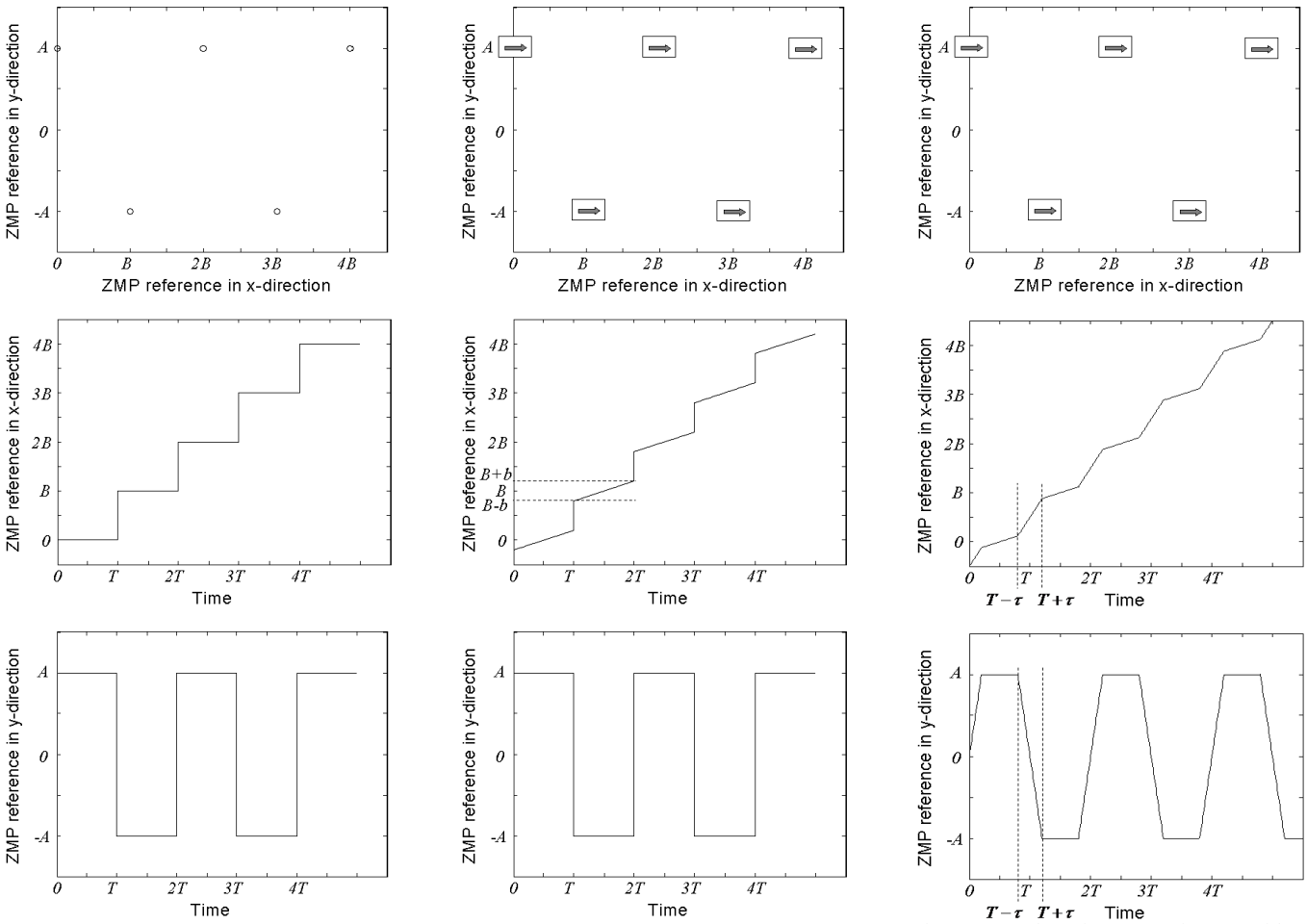

Fig. 2. Fixed ZMP references.

Fig. 3. Forward moving ZMP reference

Fig. 4. Forward moving ZMP references with pre-assigned double support phases.

With this motivation, in [10], a new ZMP reference trajectory is employed where the double support phase is introduced by using the parameter τ in Fig. 4. An interpolation interval is inserted around multiples of the half walking period T. The durations of the intervals are equal to 2τ and they correspond to double support periods. The description of the $p_x^{ref}(t)$ in Fig. 4 is given by

$$p_x^{ref} = (B/T)(t - T/2) + p_x'^{ref} \tag{3}$$

where $p_x'^{ref}$ is periodic with period T. $p_x'^{ref}$ is a combination of three line segments on [0 , T]:

$$p_x'^{ref} = \begin{cases} \Omega_1 + \sigma_1 t & \text{if} \quad 0 \le t \le \tau \\ \Omega_2 + \sigma_2 t & \text{if} \quad \tau < t \le T - \tau \\ \Omega_3 + \sigma_3 t & \text{if} \quad T - \tau < t \le T \end{cases}. \tag{4}$$

$$\Omega_1 = 0, \quad \sigma_1 = \delta/\tau, \quad \Omega_2 = \delta - \tau\sigma_2, \quad \sigma_2 = -2\delta/T - 2\tau,$$
$$\Omega_3 = -\delta - (T - \tau)\sigma_3, \quad \sigma_3 = \sigma_1. \tag{5}$$

with

$$\delta = (T - 2\tau/T)(B/2 - b). \tag{6}$$

Note that δ is the magnitude of peak difference between p_x^{ref} and the non-periodic component $(B/T)(t - T/2)$ of p_x^{ref}. $p_y^{ref}(t)$ in Fig. 4 is expressed as

$$p_y^{ref} = \sum_{k=1}^{\infty} \mathrm{A}(-1)^k \{ (2/2\tau)(t - kT)[u(t - (kT - \tau)) - u(t - (kT + \tau))] + [u(t - (kT + \tau)) - u(t - (kT + T - \tau))] \}, \tag{7}$$

where $u(\cdot)$ represents the unit step function.

Defining $\omega_n \equiv \sqrt{g/z_c}$, we can rewrite (1) and (2) for the reference variables as follows.

$$\ddot{c}_x^{ref} = \omega_n^2 c_x^{ref} - \omega_n^2 p_x^{ref}, \tag{8}$$

$$\ddot{c}_y^{ref} = \omega_n^2 c_y^{ref} - \omega_n^2 p_y^{ref}. \tag{9}$$

Note that the y-direction ZMP reference $p_y^{ref}(t)$ is a periodic function with the period $2T$. It is reasonable to assume that $c_y^{ref}(t)$ is periodic too and that it has the same period. Hence, it can be approximated by a Fourier series

$$c_y^{ref}(t) = \frac{a_0}{2} + \sum_{k=1}^{\infty} a_k \cos(\frac{2\pi kt}{2T}) + b_k \sin(\frac{2\pi kt}{2T}). \tag{10}$$

By (9) and (10), p_y^{ref} can be expressed as

$$p_y^{ref}(t) = c_y^{ref} - \frac{1}{\omega_n^2}\ddot{c}_y^{ref} \tag{11}$$

$$= \frac{a_0}{2} + \sum_{k=1}^{\infty} a_k (1 + \frac{\pi^2 k^2}{\omega_n^2 T^2}) \cos(\frac{2\pi kt}{2T}) + b_k (1 + \frac{\pi^2 k^2}{\omega_n^2 T^2}) \sin(\frac{2\pi kt}{2T})$$

Noting that this expression is in the form of a Fourier

series for $p_y^{ref}(t)$, and since $p_y^{ref}(t)$ is an odd function, we conclude that $a_0/2$ and $a_k(1+(\pi^2k^2)/(\omega_n^2T^2))$ for $k=1,2,3,\cdots$ are zero. The coefficients $b_k(1+(\pi^2k^2)/(\omega_n^2T^2))$ are computed by the Fourier integral:

$$b_k(1+\frac{\pi^2k^2}{\omega_n^2T^2})=\frac{2}{2T}\int_0^{2T}p_y^{ref}\sin(\frac{2\pi kt}{2T})dt \tag{12}$$

As a result, after some arithmetical steps (omitted here), the coefficients b_k of $c_y^{ref}(t)$ in (10) can be obtained as

$$b_k=\begin{cases}\dfrac{\omega_n^2T^2}{\omega_n^2T^2+\pi^2k^2}\dfrac{2A}{\pi k}\left\{\left[\dfrac{2}{\tau}\left\langle\dfrac{T}{\pi k}\sin(\dfrac{\pi k\tau}{T})-\tau\cos(\dfrac{\pi k\tau}{T})\right\rangle\right]\right. \\ \qquad\left.+\left[\cos(\dfrac{\pi k\tau}{T})-\cos(\dfrac{\pi k(T-\tau)}{T})\right]\right\} \text{ if } k \text{ is odd} \\ 0 \quad \text{if } k \text{ is even}\end{cases} \tag{13}$$

The second step is finding the Fourier series coefficients for c_x^{ref}. In Fig. 4, p_x^{ref} is not a periodic function. It cannot be expressed as a Fourier series. However, as expressed above, this function is composed of the periodic function $p_x'^{ref}$ and the non-periodic function $((B/T)(t-T/2))$.It is again a reasonable assumption that c_x^{ref} has a periodic part and a non-periodic part too. Further, if we suppose that the two non-periodic parts (of $p_x^{ref}(t)$ and c_x^{ref}) are non-equal, then the difference $p_x^{ref}(t)-c_x^{ref}$ will be non-periodic. This is not expected in a continuous walk as the one described in Fig. 4. Therefore we conclude that the non-periodic parts of the two functions are equal. Note that, the period of the periodic part of $p_x^{ref}(t)$ is T and we can state the same for the period of the periodic part of c_x^{ref}. Finally, c_x^{ref} can be expressed as the sum of the non-periodic part of p_x^{ref} and a Fourier series:

$$c_x^{ref}=\frac{B}{T}(t-\frac{T}{2})+\frac{\alpha_0}{2}+\sum_{n=1}^{\infty}\alpha_k\cos(\frac{2\pi nt}{T})+\beta_k\sin(\frac{2\pi nt}{T}) \tag{14}$$

With (8) and (14) $p_x^{ref}(t)$ as a Fourier series is

$$p_x^{ref}(t)=c_x^{ref}-(1/\omega_n^2)\ddot{c}_x^{ref}=(B/T)(t-T/2)+\alpha_0/2 \tag{15}$$
$$+\sum_{n=1}^{\infty}\alpha_k(1+\frac{\pi^2k^2}{\omega_n^2T^2})\cos(\frac{2\pi kt}{T})+\beta_k(1+\frac{\pi^2k^2}{\omega_n^2T^2})\sin(\frac{2\pi kt}{T})$$

Therefore the Fourier coefficients of $p_x'^{ref}(t)$, the periodic part of $p_x^{ref}(t)$, are $\alpha_0/2$, $\alpha_k(1+\pi^2k^2/\omega_n^2T^2)$ and $\beta_k(1+\pi^2k^2/\omega_n^2T^2)$ for $k=1,2,3,\cdots$ The Fourier coefficients $\alpha_0/2$, $\alpha_k(1+\pi^2k^2/\omega_n^2T^2$ of $p_x'^{ref}(t)$ are zero because this is an odd function. The coefficients for $\beta_k(1+(\pi^2k^2)/(\omega_n^2T^2))$ can be found by

$$\beta_k(1+\pi^2k^2/\omega_n^2T^2)=\frac{2}{T}\int_0^T p_x'^{ref}(t)\sin(\frac{2\pi kt}{T})dt\,. \tag{16}$$

This yields the result

$$\beta_k=\frac{\omega_n^2T^2}{\pi^2k^2+\omega_n^2T^2}\frac{2}{\pi k}\left\{\sigma_1\left[-\tau\cos(\frac{2\pi k\tau}{T})+\frac{T}{2\pi k}\sin(\frac{2\pi k\tau}{T})\right]\right. \tag{17}$$
$$\left.+\sigma_2\left[\tau\cos(\frac{2\pi k\tau}{T})-\frac{T}{2}\left(\cos\left(\frac{2\pi k\tau}{T}\right)\right)-\frac{T}{2\pi k}\sin(\frac{2\pi k\tau}{T})\right]\right\}.$$

The curves obtained for c_x^{ref} and c_y^{ref} are shown in Fig. 5 together with the corresponding ZMP references defined in Fig. 4. The infinite sums in (10) and (14) are approximated by finite sums of N terms. $N=24$ is used in the experiments. N is found by the inspection of the "Fourier-series-approximated" p_y^{ref} and p_x^{ref} curves obtained from (11) and (15) respectively. (These approximated curves are not shown here due to space considerations. These curves, however, are computed, plotted and compared with the ZMP references in Fig. 4. in order to validate the formulae derived for the Fourier series coefficients. The plots served a secondary purpose of determining a suitable value for N too.) We observed that, with $N=24$, the approximated curves match with the original piecewise continuous ZMP reference curves in Fig. 4. The matching quality we judged from the reproduction of the sharp corners of the original ZMP reference curves in their approximated versions. With lower values for N the matching quality is deteriorated. In Fig 5, the following parameter values are used: $A=0.1$ m, $B=0.1$ m, $b=0.04$ m, $T=1$ s and $\tau=0.2$ s.

In addition to the CoM references, foot position reference trajectories have to be designed too. The x and z-direction components of the foot trajectories used in this paper are shown in Fig. 6. These curves are combinations of sinusoidal and constant function segments. T_d and T_s represent the double and single support periods, respectively. ($T_d=2\tau$, $T_s=T-\tau$.) B is the step size from Fig. 4. The y direction trajectories are constant at $-A$ and A for the right and left feet, respectively, where A is half of the foot to foot y direction distance also shown in Fig. 4. h_s is the step height parameter and h_p is the ground push magnitude. The foot orientation references used in inverse kinematics are computed for feet parallel to the ground.

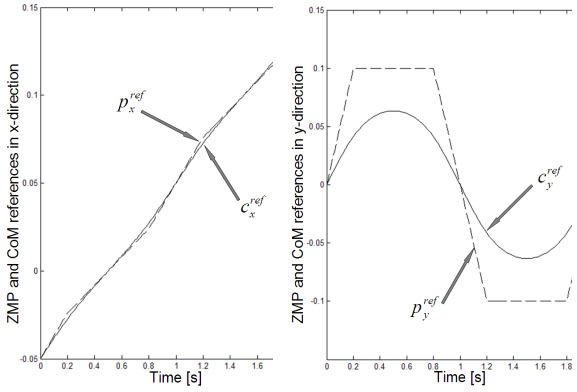

Fig. 5. x and y-direction CoM and ZMP references

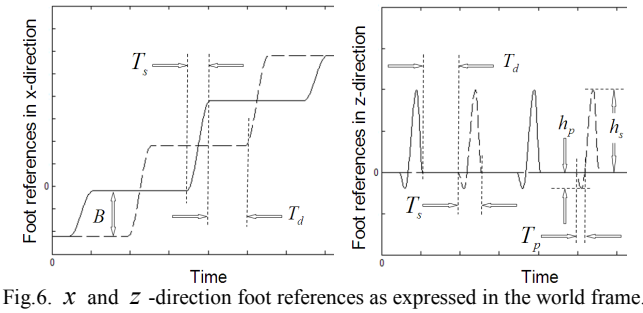

Fig.6. x and z -direction foot references as expressed in the world frame. Solid curves belong to the right foot, dashed curves indicate left foot.

III. Control Algorithm

The walking control method used in this paper follows the control approach presented in [12]. Firstly, the joint position references are generated through inverse kinematics from CoM and swing foot references defined in world frame coordinates and obtained in the previous section. Independent PID controllers are used for joint position control. A set of compensators are then employed during the walk for the balance and foot-ground interaction enhancements. A block diagram of the controllers used is shown in Fig. 7.

IV. Experimental Results

In this section, a brief introduction of the bipedal humanoid robot SURALP is given and experimental results are presented. A picture and dimensional drawings of the robot are shown in Figures 8 and 9, respectively. It is designed in human proportions with 29 DOF, including 6-DOF legs, 6-DOF arms, 1 DOF hands, a 2-DOF neck and a 1-DOF waist. The weight of the robot is 114 kg. DC motors are used as actuators. Belt-pulley systems transmit the motor rotary motion to Harmonic Drive reduction gears. The sensor system of SURALP includes encoders measuring the motor angular positions, six-axes force/torque sensors are positioned at the ankles and wrists, a rate gyro, an inclinometer, and a linear accelerometer which are mounted at the robot torso. The control hardware of SURALP consists of a modular dSpace digital signal processing system in a backpack configuration. Motor drivers are in the trunk.

In the experiments, SURALP successfully walked with the generated reference trajectories based on forward moving natural ZMP trajectories and the control algorithms in [12]. The video attachment shows typical robot walk with side and front views. Reference generation parameters used are given in Table I. The reference and actual ZMP curves on the ground surface for a five step walk are shown in Fig. 10. It can be observed that the overall shape of the ZMP reference curve is followed by the actual ZMP. However, the actual curve first leads and later lags the reference. The reason for the lead is that there is an initial offset between the two curves. Such offsets may result from surface irregularities. The reason for the lag is early landings of the swing foot. The early landing foot reference modification method in the x-direction, as explained in [12], "crops" swing foot x-references and causes the accumulation of ZMP error with the increasing number of steps taken. However, this does not cause the robot to loose balance. This is because the reference generation method creates body-frame foot references from the difference of the world-frame CoM and foot position references. An early landing swing foot reference x-directional crop causes the lag of both the CoM and the feet behind their references, by the same amount. Therefore, the originally planned body frame references can still be used although the robot is behind its reference as described in the world frame. Fig. 11 shows the body roll and pitch angles during an eleven step walk. With the continuous and natural ZMP based reference trajectory, in this experiment, stability of the walk is improved significantly when compared to the experiments with SURALP in [12] where the walking references were not ZMP based but are generated as combinations of sinusoidal and linear functions in an ad-hoc manner. A walk with 12 cm step size is achieved while maximum step size was 6 cm in the previous works with this robot.

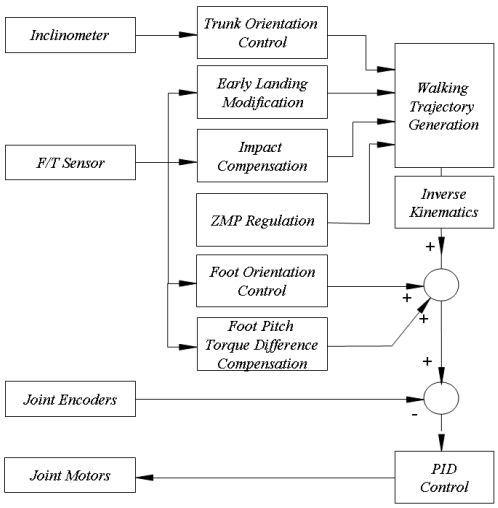

Fig. 7. The control block diagram [12].

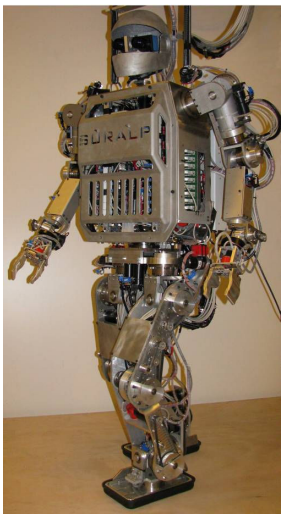

Fig. 8. Humanoid robot SURALP

As it is seen from this figure, the body roll angle oscillates between +2.5deg to -3.5 deg and the body pitch angle oscillates between +2.1 to -1.7. Oscillations in these ranges are quite acceptable for a bipedal robot whose upper body is much heavier than the legs which are traveling a 24 cm distance in the swing phase.

V. Conclusion

In this paper, a forward moving continuous Zero Moment Point based reference trajectory generation is implemented for a stable and human-like walk of the bipedal humanoid robot SURALP. The relation between the Zero Moment Point and the robot Center of Mass coordinates is obtained via the Linear Inverted Pendulum Model. In order to obtain the Center of Mass reference trajectory, ZMP reference trajectories are approximated with Fourier series. Continuous nature of the ZMP reference trajectories provides non-oscillatory references, so that the smoothing with Lanczos sigma factors are not necessary unlike it is the case in [8]. Single support and double support phase durations are introduced as predefined separate parameters. Experimental results show that the generated stable human-like ZMP reference trajectory successfully enables a stable bipedal walk with a step size of 12 cm.

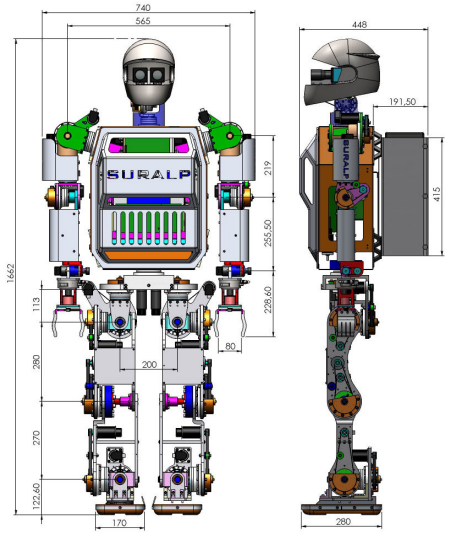

Fig. 9. SURALP, dimensions.

TABLE I
Reference Generation Parameters

Symbol	Definition	Value
T_s	Single support period	1 s
T_d	Double support period	0,9 s
T_p	Push period	0.4 s
A	ZMP reference in y direction	7 cm
$2b$	ZMP motion under the sole	4 cm
B	Step size	12 cm
h_s	Step height	1.5 cm
h_p	Ground push magnitude	1 cm

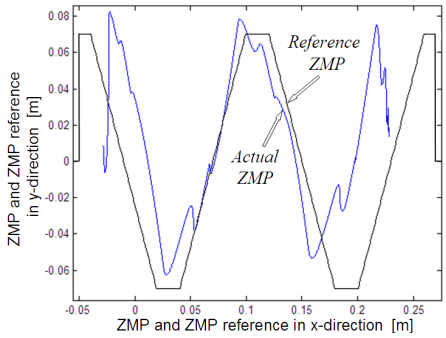

Fig. 10. ZMP and ZMP reference on the x-y-plane.

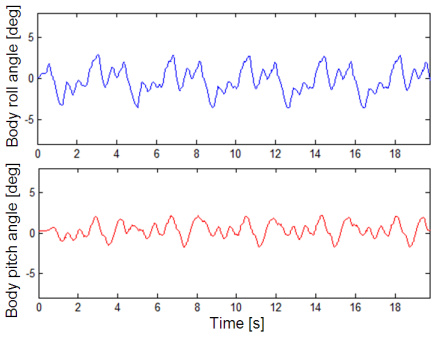

Fig. 11. Body roll and pitch angles

References

[1] M. Vukobratovic, B. Borovac, D. Surla and D. Stokic, *Biped Locomotion: Dynamics, Stability and Application*. Springer, 1990.

[2] S. Kajita, K. Kaehiro, K. Kaneko, K. Fujiwara, K. Yokoi, and H. Hirukawa, "A real time pattern generator for bipedal walking" *Proc. IEEE Int. Conf.on Robotics and Aut.,* vol.1, pp.31-37, May 2002.

[3] S. Kajita, F. Kahehiro, K. Kaneko, K. Fujiwara, K. Harada, K. Yokoi, H. Hirukawa, " Biped walking pattern generation using preview control of the zero-moment-point", *IEEE Int. Conf. on Robotics and Automation, pp: 1620 - 1626, vol.2*, Taipei, Taiwan, September 2003.

[4] Y. Choi, B. J. You, and S. R. Oh, "On the stability of indirect ZMP controller for biped robot systems", *Proc. of Int. Conf. on Intelligent Robots and Systems, pp: 1966-1971, vol.2*, Sendal, Japan, June 2004.

[5] A. Dasgupta, and Y. Nakamura, "Making feasible walking motion of humanoid robots from human motion capture data" *Proc. IEEE Int. Conf. on Robotics and Automation*, Detroit, Michigan, May 1999.

[6] K. Erbatur, A. Okazaki, K. Obiya, T. Takahashi and A. Kawamura, "A study on the zero moment point measurement for biped walking robots", *Proc. 7th Int. Workshop on Adv. Motion Control, pp. 431-436*, Maribor, Slovenia, 2002

[7] C. Zhu, Y. Tomizawa, X. Luo, and A. Kawamura "Biped walking with variable ZMP, frictional constraint, and inverted pendulum model", *IEEE Int. Conf. on Robotics and Biomimetics, pp: 425 – 430*, Shenyang, China Aug 2004.

[8] K. Erbatur and O. Kurt, "Natural ZMP Trajectories for Biped Robot Reference Generation", *IEEE Trans. Industrial Electronics*, vol. 56, no. 3, pp. 835-845, March 2009.

[9] A. Takanishi, H. Lim, M. Tsuda and I. Kato. "Realization of dynamic biped walking stabilized by trunk motion on a sagittally uneven surface," *IEEE/RJS Int. Conf. on Intelligent Rob. and Syst.*, 1990.

[10] K. Erbatur, O. Koca, E. Taşkıran, M. Yılmaz and U. Seven., "ZMP Based Reference Generation for Biped Walking Robots" *ICICRA'09, Int. Conf. Intelligent Control, Rob. and Aut.*, Venice, Italy, Oct. 2009.

[11] K. Erbatur, U. Seven U., E. Taşkıran, Ö. Koca., G. Kızıltaş., M. Ünel, A. Sabanovic and A. Onat, "SURALP-L, The Leg Module of a New Humanoid Platform," *Proc. of the 2008 IEEE/RAS Int. Conf. on Humanoid Robots*, pp. 168-173, Daejeon, Korea, December 2008.

[12] K. Erbatur, U. Seven, E. Taşkıran, Ö. Koca M. Yılmaz, M. Ünel, G. Kızıltaş, A. Sabanovic and A. Onat, "SURALP: A New Full-Body Humanoid Robot Platform" *Proc. IROS 2009 - IEEE/RSJ Int. Conf. on Intelligent Robots and Systems*, St. Louis, MO, USA, Oct. 2009.